

SUPPLEMENTAL MATERIAL

MATERIAL AND METHODS

Mouse Exercise Testing and Blood Lactate Measurements

Maximum duration of swimming exercise was measured in a temperature-controlled (34°C), adjustable-current tank as previously described.¹ Briefly, mice were acclimated to swimming for 10 min/day for 3 d and swimming duration measured to the point of exhaustion. For graded maximal treadmill exercise, mice were acclimated by running for 10 min at 10 m/min for 3 d and maximum exercise capacity determined by graded increase in treadmill speed (10, 12 and 15 m/min for 3-5 min at each speed followed by 1.8 m/min increase every 3 min) on a 10% incline to exhaustion. Work (J) = Force (body weight (kg) X 9.8 m/sec²) X Vertical distance (sin (5°) x speed (m/min) x time (min)). Exercise training was initiated in 8 week-old mice at 10 m/min for 40 min on a 6-lane treadmill and gradually increased to 14 m/min for 90 min, 5 d/wk for 5 wk (final age ~14 wk old). For high intensity exercise, mice were treadmill acclimated for 3 d and sprint capacity determined by rapid ramping speed protocol (1 m/min every 30 sec on a 10% incline) to exhaustion. Blood lactate levels at rest and after sub-maximum (~70% of p53+/+ capacity, ~22 min) exercise were measured using the LactatePro analyzer (Arkray).

Body Mass Composition

Body composition (muscle, fat and free fluid) was measured in non-anesthetized mice using the Bruker Minispec NMR analyzer mq10 (Bruker Optics).²

Assessment of Cardiac Function by Dobutamine MRI

Cardiac MRI was performed at rest and during dobutamine stress. Mice were anesthetized with isoflurane, placed prone on a plastic cradle, head stabilized with a holder-bite bar and nosecone for isoflurane delivery, hydrated with subcutaneous 0.9% saline (~0.5-1 ml/25 g mouse), and monitored with a pressure transducer for respiration and rectal temperature probe. Conductive leads were placed for ECG acquisition. The mouse cradle and apparatus were placed in a volume MR coil with warm air blower for body temperature control. A contrast agent (Gd-DTPA, Berlex) was delivered at 0.3 mmol/kg i.v. by tail vein cannulation. Short axis cine cardiac MRI scans were obtained: repetition time 9-10 ms, echo time 3.4 ms, 4-5 averages, 10 or more frames depending on heart rate. Cine scans were obtained on 3 slices at mid-ventricle at baseline and during dobutamine stress. Dobutamine was administered in two steps at 10 and 40 µg/kg/min by tail vein catheter. Ejection fractions were calculated for baseline and stress steps using CAAS_MRV_FARM software (Pie Medical Imaging, Netherlands).

Neuromuscular and Strength Testing

Motor coordination was assessed by latency to fall using the rotarod (Rota-Rod, UGO Basile). Rotarod performance was measured for four consecutive days with four trials per day. Rotating rod speed was gradually increased from 2-20 rpm or 4-40 rpm and endpoint was time to fall or up to 600 sec.

As a general assessment of skeletal muscle strength, mouse forelimb grip strength was assessed by using a digital grip strength meter (Columbus Instruments). Mice were acclimated for two consecutive days prior to the experiment days. Each mouse was held by the tip of the tail and lowered toward the grip triangle bar and was allowed to grasp it with its forepaws. The mouse was then pulled steadily by the tail away from the triangle bar until the mouse's grip was broken. The force exerted on the gauge at the time the grip was broken was recorded from the strength meter. Each mouse was given three trials approximately 10 min apart. This was repeated the next day and the results were an average of the two days for a total of six trials.³

Muscle Fiber Typing and Capillary Density by Immunofluorescence

Muscle tissue was frozen in Tissue-Tek OCT compound (Sakura Finetek) by placing on partially frozen isopentane in liquid nitrogen. Muscle sections (8 μm) were cut using a cryostat (Leica). For muscle fiber typing, tissue sections were fixed in 4% paraformaldehyde for 15 min, permeabilized in 0.1% Triton X-100 for 20 min and incubated with goat polyclonal antibodies against MHC I (slow) or MHC II (fast) fibers (Novocastra) at room temperature.

To assess for capillary density, tissue sections were fixed in 0.4% paraformaldehyde for 10 min, permeabilized in 0.1% Triton-X for 20 min and incubated with anti-mouse CD31 antibody (BD Pharmingen). Secondary antibodies conjugated to Alexa Fluor 594 (Molecular Probes) were used for visualization of primary antibody binding.⁴

Peak Vo_2 and Respiratory Exchange Ratio (RER)

Peak Vo_2 and RER were measured using indirect calorimetry with single-lane sealed treadmill apparatus (Columbus Instruments) as previously described.⁵ The calorimeter was calibrated before each testing session using standard gases (20.5% O_2 and 0.5% CO_2) and air flow rate through the sealed treadmill was set at 0.6 L/min. Mice were acclimated to the sealed treadmill for 3 days. After 5 min of baseline gas collection, the maximum exercise protocol was initiated at 10 m/min at 10% incline with a graded increase in speed by 1 m/min every 1.5 min until exhaustion. Peak Vo_2 was defined as O_2 consumption at maximum exercise per kg body mass per h (ml/kg/h). O_2 consumption and CO_2 production were collected every 30 seconds during exercise to calculate the RER.

Mitochondria Purification and Oxygen Consumption

After mice were euthanized and perfused with ice-cold PBS, skeletal muscle mitochondria were isolated using standard protocols as described.⁶ Oxygen consumption was measured using a Clark-type oxygen microelectrode at 30°C as previously described.⁷ Respiration was initiated by adding 10 mM glutamate, 2 mM malate and 0.8 mM ADP. Final oxygen consumption was adjusted to the weight of skeletal muscle tissue to reflect differences in mitochondrial content (nmol O_2 /min/g tissue).

Antibodies and Western Blotting

Antibodies were from the following sources: rabbit control IgG serum (SC-2027), rabbit polyclonal anti-p53 (against full-length protein, FL-393, SC-6243), goat polyclonal anti-TFAM (A-17) (Santa Cruz Biotech); rabbit polyclonal anti-PGC-1 α (101707, Cayman); rabbit polyclonal anti-p53R2 (Abcam); rabbit polyclonal anti-SCO2 as described⁸; rabbit polyclonal anti-TFAM (a generous gift from Dr. Eric A. Shoubridge, McGill University), and mouse monoclonal anti-tubulin (Clone B-5-1-2, Sigma) antibodies. Proteins samples were homogenized in ice cold RIPA lysis buffer with protease inhibitor cocktail (Roche), resolved by Tris-glycine SDS PAGE, and transferred to Immobilon-P membrane (Millipore) for standard ECL western blotting.

Histochemistry

Glycogen was detected in 10% formalin fixed tissue sections with periodic acid Schiff staining using a PAS stain kit (Polysciences) with and without diastase digestion. Acidified Harris hematoxylin was used as a counterstain. Succinate dehydrogenase staining was performed using nitro blue tetrazolium in frozen tissue sections as previously described.⁹ For all histochemical techniques, the p53+/+ and p53-/- muscle sections were placed on the same glass slide, thus, all pairs underwent identical incubation conditions and washes.

Electron Microscopy

Muscle tissue was fixed with glutaraldehyde and paraformaldehyde, post-fixed with osmium tetroxide, stained *en block* with uranyl acetate, ethanol dehydrated and Epon embedded

(Electron Microscopy Sciences). 60 nm thick sections were cut on a Sorvall MT2 ultra-microtome, stained with uranyl acetate and lead citrate and viewed with a JEM 1200 EXII electron microscope (JEOL USA) equipped with an AMT XR-60 digital camera (Advanced Microscopy Techniques). The volume density of mitochondria was estimated using the point-counting method.^{10,11}

Chromatin Immunoprecipitation (ChIP) Assay Primer Sequences

The genomic locations (relative to bp +1 position of the ATG start site) of the putative p53 responsive elements (p53REs) in the *TFAM* gene are as follows: p53RE-1, +2475 to +2497; p53RE-2, +6538 to +6568; p53RE-3, +7087 to +7110; and p53RE-4, +11631 to 11657. Real-time PCR primer pair sequences:

TFAM p53RE-1 (intron 3) nonspecific control,

Forward (F) 5'-GCTTCCTGACAGTTGTGTAGATAGGG-3'

Reverse (R) 5'-GCCTGCGAATGCTCAGGGTC-3';

TFAM p53RE-3 (intron 5),

F (+7017 to +7037) 5'-CTGCAAACACCCACCCAGAC-3',

R (+7197 to +7172) 5'-CTATGTGGGGGTATACTGCTGAC-3';

APOE nonspecific control,

F 5'-GCCTAGCCGAGGGAGAGCCG-3',

R 5'-TGTGACTTGGGAGCTCTGCAGC-3';

p21 p53RE,

F (-7600 to -7580) 5'-GCAAGGCTGCATCAGTCCTCC-3',

R (-7351 to -7373) 5'-GGTCTCTGTCTCCATTCATGCTC-3'.

Real-time PCR mRNA Quantification

Total RNA was isolated from tissues using the RNeasy Kit (QAIGEN), cDNA synthesized on poly-dT magnetic beads by reverse transcription (Superscript II, Invitrogen) and quantified by real-time RT-PCR using SYBR green fluorescence on the 7900HT Sequence Detection System (Applied Biosystems) as previously described.¹² Cycle threshold (Ct) values were normalized to the housekeeping gene eukaryotic translation initiation factor *EIF35S* (TIF). Primer sequences are provided below:

TIF,

F 5'-CTGAGGATGTGCTGTCTGGGAA-3',

R 5'-CCTTTGCCTCCACTTCGGTC-3';

TFAM,

F 5'-CTGATGGGTATGGAGAAGGAGG-3',

R 5'-CCAACCTCAGCCATCTGCTCTTC-3';

p53R2,

F 5'-CCAGGTTACCATGGTTGTGG-3',

R 5'-CCAGTGCACTCAGTAGCTGTG-3';

SCO2,

F 5'-CAGCCTGTCTTCATCACTGTGGA-3',

R 5'-GACACTGTGGAAGGCAGCTATGTGCC-3';

FDXR,

F 5'-CCATGACAGACAGCTTCCTCAC-3',

R 5'-CAGCAGCCGCAGCATCTCTC-3';

TIGAR,

F 5'-ACTGAGAAGCAGCACTGAGTGTG-3',

R 5'-CGGATGTGCAAGCCTCAATGTC-3';

PGC-1 α ,

F 5'-ACGGTTTACATGAACACAGCTGC-3',
R 5'-CTTGTTTCGTTCTGTTTCAGGTGC-3';
PGC-1 β ,
F 5'-ATACCTCAGACAAGGCCCTTCC-3',
R 5'-ACAGAAGGAAGTCAGTCGGGTG-3'.
NRF1,
F 5'-GAACGCCACCGATTTCACTGTC-3',
R 5'-CCCTACCACCCACGAATCTGG-3';
NRF2,
5'-GGCACAGTGCTCCTATGCGTG-3',
5'-CCAGCTCGACAATGTTCTCCAGC-3';
CYCS,
F 5'-TTGACCAGCCCGGAACGAAT-3'
R 5'-GCTATTAGGTCTGCCCTTTCTCCC-3'
COX4i1,
F 5'-CGAGAGCTTCGCCGAGATGAAC-3',
R 5'-GCAGCTTCCAGCATGCCGAGG-3'
ND1,
F 5'-AATCGCCATAGCCTTCCTAACAT-3',
R 5'-GGCGTCTGCAAATGGTTGTAA-3';
COX2 (MTCO2),
F 5'-CCATAGGGCACCAATGATACTG-3'
R 5'-AGTCGGCCTGGGATGGCATC-3'

mtDNA Content Quantification

Mitochondrial DNA was co-purified with genomic DNA from mouse tissues using the DNeasy kit (QIAGEN), Ct values determined for *MTCO2* gene encoded by mtDNA and 18S rRNA gene encoded by the nuclear DNA, and the relative mtDNA copy number calculated by normalizing to 18S rRNA gene copy number.¹³ Primer sequences for *MTCO2* and 18S rRNA are provided below:

MTCO2,
F 5'-CCATAGGGCACCAATGATACTG -3',
R 5'-AGTCGGCCTGGGATGGCATC-3';
18S rRNA,
F 5'-CTTAGAGGGACAAGTGGCGTTC-3';
R 5'-CGCTGAGCCAGTCAGTGTAG-3'.

shRNA Sequences

Non-specific shRNA,
5'-ccggCAACAAGATGAAGAGCACCAActcgagttggtgctcttcatcttgtgtttt-3',
TFAM-specific shRNA,
5'-ccggCGGAGACATCTCTGAGCATTActcgagtaatgctcagagatgtctccgttttg-3'.

ONLINE FIGURE LEGENDS

Online Figure I.

Muscle glycogen content is unaffected by *p53* genotype. Glycogen was stained using the PAS method on *p53*^{+/+} and *p53*^{-/-} soleus (SOL), tibialis anterior (TA), and gastrocnemius (GAS) with (+Diastase, right panel) or without (left panel) glycogen digestion using diastase. Magnification, 20X.

Online Figure II.

Morphology and body mass composition are similar in *p53*^{+/+} and *p53*^{-/-} mice. A, Morphology of 10-week old age-matched male *p53*^{+/+} and *p53*^{-/-} littermates (C57BL6/J background). B, Body mass (g) of *p53*^{+/+} and *p53*^{-/-} mice, n = 5 each. C, Body mass composition (muscle, fat and free fluid) of *p53*^{+/+} (dark) and *p53*^{-/-} (light) mice determined by NMR in non-anesthetized age- and sex-matched littermates, n = 5 each. *P*-values were non-significant; data shown as mean \pm SEM.

Online Figure III.

Decreased mitochondrial density in *p53*^{-/-} mouse soleus muscle. A, Representative images of transmission electron micrographs of intermyofibrillar mitochondria in *p53*^{+/+} and *p53*^{-/-} mouse soleus muscles. Upper panel, 15000X; lower panel, 5000X. Scale bars, 1 μ m. B, Estimated relative volume density of mitochondria. ***P* < 0.01; n=3. Data shown as mean \pm SEM.

Online Figure IV.

p53R2, *SCO2*, *FDXR* and *TIGAR* expression levels are unchanged by *p53* genotype. A, *SCO2* mRNA (left panel) and protein (right panel) expression levels in soleus of *p53*^{+/+} and *p53*^{-/-} mice. B, Relative *p53R2* mRNA levels in soleus, heart and liver by RT-PCR. C, *p53R2* protein expression in soleus, heart and liver tissues by western blotting. D, Relative *FDXR* (left panel) and *TIGAR* (right panel) mRNA levels. Tubulin levels are shown as protein loading control (A and C). *p53*^{+/+} (dark) and *p53*^{-/-} (light) mice; data shown as mean \pm SEM.

Online Figure V.

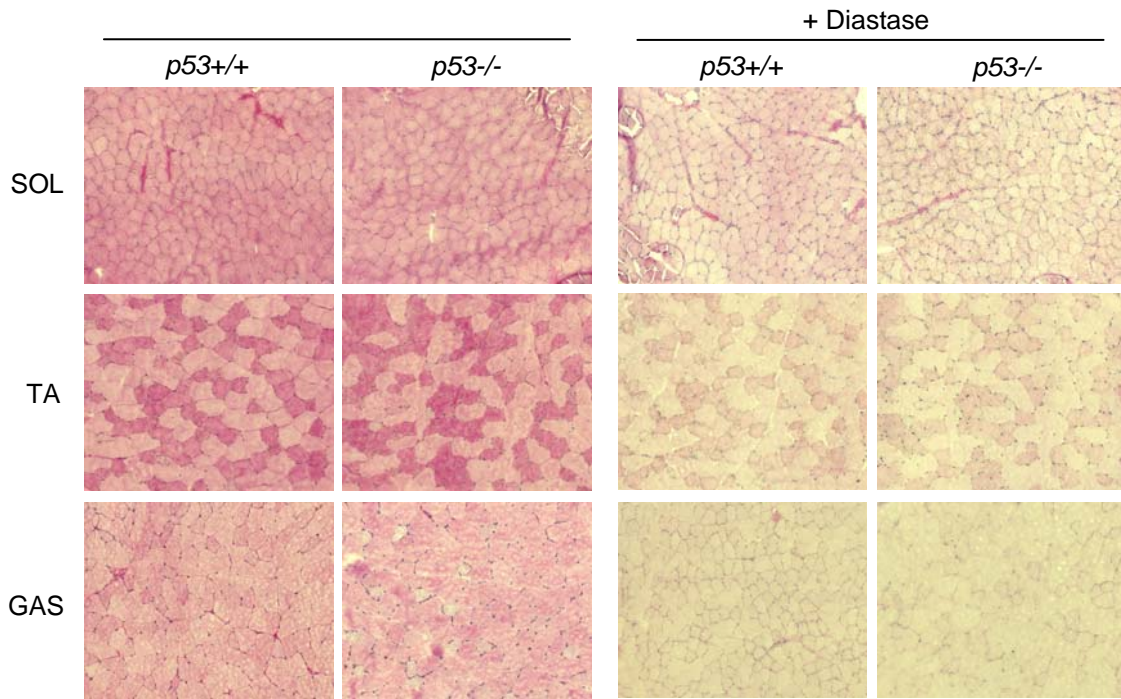
PGC-1 α , other mitochondrial biogenesis regulators and mitochondrial respiratory subunit gene expression are not significantly affected by *p53* genotype at baseline or after acute exercise. A, Basal *PGC-1 α* protein levels detected by western blotting in soleus and gastrocnemius (Gastroc) of *p53*^{+/+} and *p53*^{-/-} mice. The positive control mouse myoblast C2C12 cell protein lysate shows a strong band at 96 kDal as specified by the manufacturer. B, Time course of *PGC-1 α* mRNA expression in response to acute exercise in *p53*^{+/+} and *p53*^{-/-} soleus muscle. C, *PGC-1 β* , other biogenesis regulators, and representative nuclear and mitochondrial genome-encoded component mRNA levels are not significantly affected by *p53* genotype at baseline or after acute exercise. **P* < 0.05 versus *p53*^{+/+} pre-exercise; n = 3. *p53*^{+/+} (dark) and *p53*^{-/-} (light) mice; data shown as mean \pm SEM.

REFERENCES

1. Matsumoto K, Ishihara K, Tanaka K, Inoue K, Fushiki T. An adjustable-current swimming pool for the evaluation of endurance capacity of mice. *J Appl Physiol*. 1996;81:1843-9.
2. Heron-Milhavet L, Haluzik M, Yakar S, Gavrilova O, Pack S, Jou WC, Ibrahimi A, Kim H, Hunt D, Yau D, Asghar Z, Joseph J, Wheeler MB, Abumrad NA, LeRoith D. Muscle-specific overexpression of CD36 reverses the insulin resistance and diabetes of MKR mice. *Endocrinology*. 2004;145:4667-76.
3. Whittemore LA, Song K, Li X, Aghajanian J, Davies M, Girgenrath S, Hill JJ, Jalenak M, Kelley P, Knight A, Maylor R, O'Hara D, Pearson A, Quazi A, Ryerson S, Tan XY, Tomkinson KN, Veldman GM, Widom A, Wright JF, Wudyka S, Zhao L, Wolfman NM. Inhibition of myostatin in adult mice increases skeletal muscle mass and strength. *Biochem Biophys Res Commun*. 2003;300:965-71.
4. Mason SD, Rundqvist H, Papandreou I, Duh R, McNulty WJ, Howlett RA, Olfert IM, Sundberg CJ, Denko NC, Poellinger L, Johnson RS. HIF-1alpha in endurance training: suppression of oxidative metabolism. *Am J Physiol Regul Integr Comp Physiol*. 2007;293:R2059-69.
5. Wende AR, Schaeffer PJ, Parker GJ, Zechner C, Han DH, Chen MM, Hancock CR, Lehman JJ, Huss JM, McClain DA, Holloszy JO, Kelly DP. A role for the transcriptional coactivator PGC-1alpha in muscle refueling. *J Biol Chem*. 2007;282:36642-51.
6. Frezza C, Cipolat S, Scorrano L. Organelle isolation: functional mitochondria from mouse liver, muscle and cultured fibroblasts. *Nat Protoc*. 2007;2:287-95.
7. McLeod CJ, Aziz A, Hoyt RF, McCoy JP, Jr., Sack MN. Uncoupling proteins 2 and 3 function in concert to augment tolerance to cardiac ischemia. *J Biol Chem*. 2005.
8. Matoba S, Kang JG, Patino WD, Wragg A, Boehm M, Gavrilova O, Hurley PJ, Bunz F, Hwang PM. p53 regulates mitochondrial respiration. *Science*. 2006;312:1650-3.
9. Pool CW, Diegenbach PC, Scholten G. Quantitative succinate-dehydrogenase histochemistry. I. A Methodological study on mammalian and fish muscle. *Histochemistry*. 1979;64:251-62.
10. Weibel ER. *Stereological Methods: Practical Methods for Biological Morphometry Vol. 1*. New York: Academic Press; 1979.
11. Sullivan SM, Pittman RN. Relationship between mitochondrial volume density and capillarity in hamster muscles. *Am J Physiol*. 1987;252:H149-55.
12. Patino WD, Mian OY, Kang JG, Matoba S, Bartlett LD, Holbrook B, Trout HH, 3rd, Kozloff L, Hwang PM. Circulating transcriptome reveals markers of atherosclerosis. *Proc Natl Acad Sci U S A*. 2005;102:3423-8.
13. D'Souza AD, Parikh N, Kaech SM, Shadel GS. Convergence of multiple signaling pathways is required to coordinately up-regulate mtDNA and mitochondrial biogenesis during T cell activation. *Mitochondrion*. 2007;7:374-85.

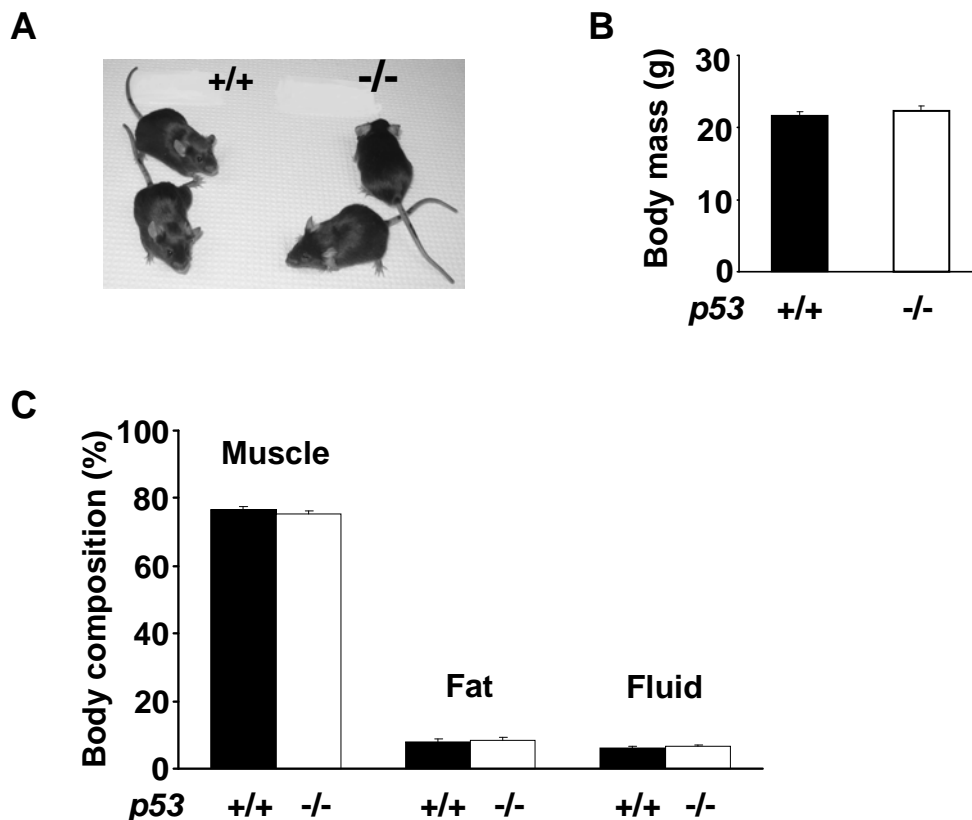
Online Figure I

Glycogen staining

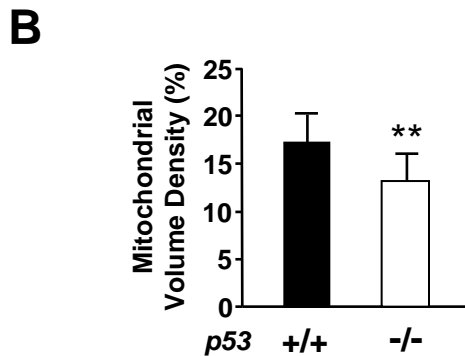
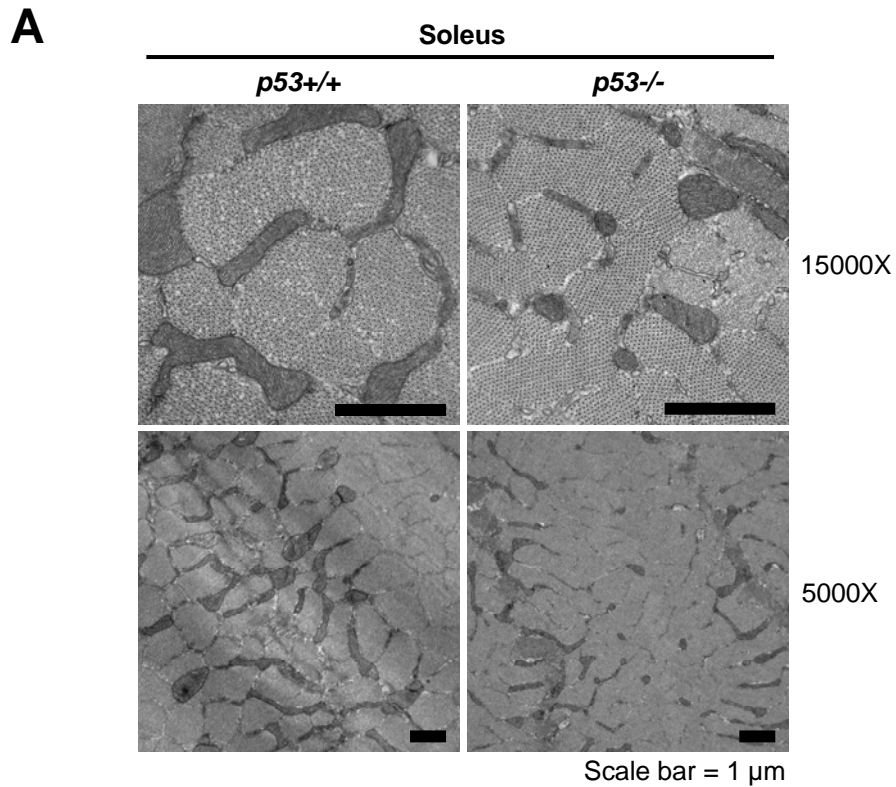


Online Figure I. Muscle glycogen content is unaffected by *p53* genotype. Glycogen was stained using the PAS method on *p53*^{+/+} and *p53*^{-/-} soleus (SOL), tibialis anterior (TA), and gastrocnemius (GAS) with (+Diastase, right panel) or without (left panel) glycogen digestion using diastase. Magnification, 20X.

Online Figure II

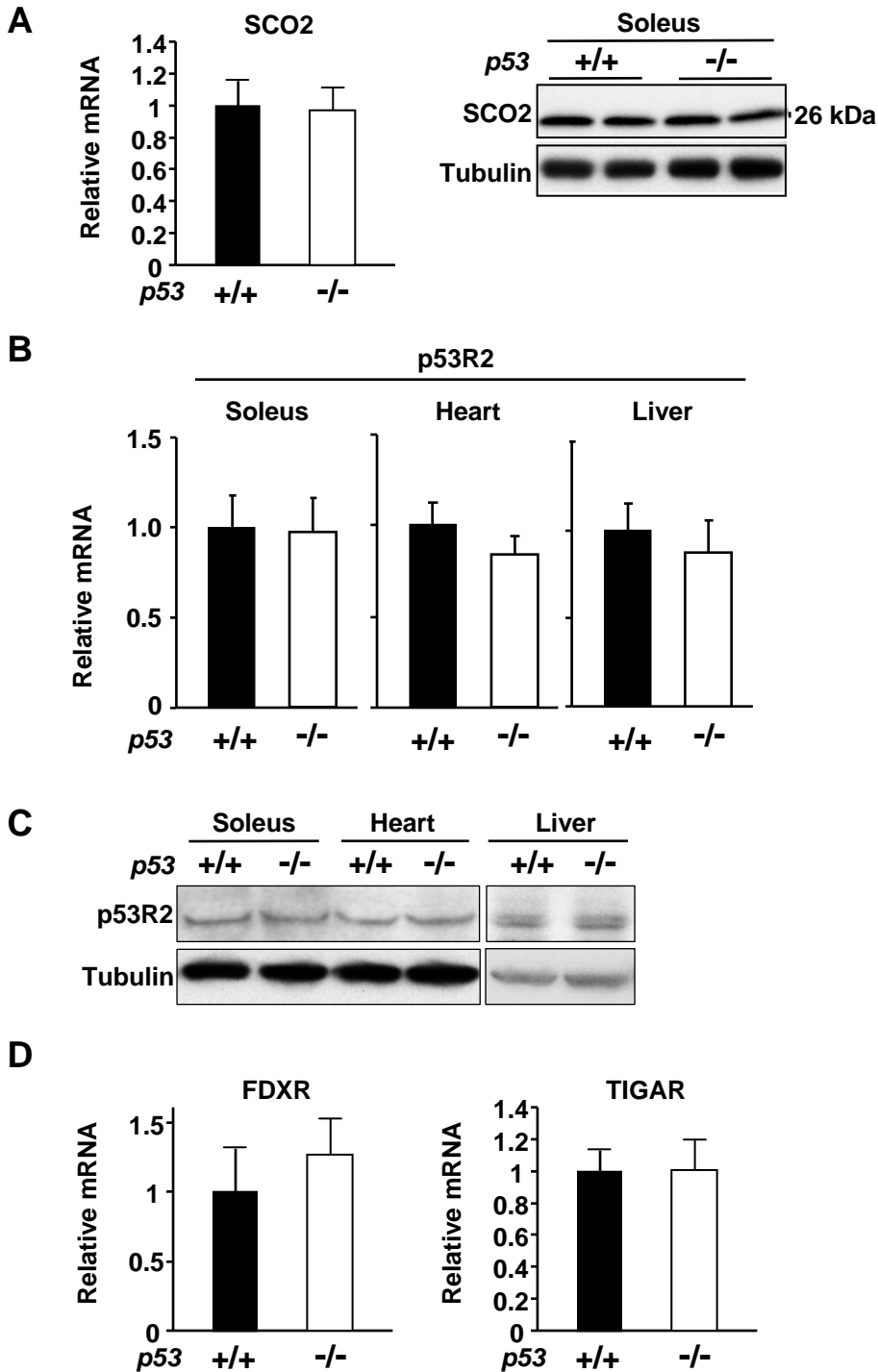


Online Figure II. Morphology and body mass composition are similar in *p53*^{+/+} and *p53*^{-/-} mice. A, Morphology of 10-week old age-matched male *p53*^{+/+} and *p53*^{-/-} littermates (C57BL6/J background). B, Body mass (g) of *p53*^{+/+} and *p53*^{-/-} mice, n = 5 each. C, Body mass composition (muscle, fat and free fluid) of *p53*^{+/+} (dark) and *p53*^{-/-} (light) mice determined by NMR in non-anesthetized age- and sex-matched littermates, n = 5 each. *P*-values were non-significant; data shown as mean \pm SEM.



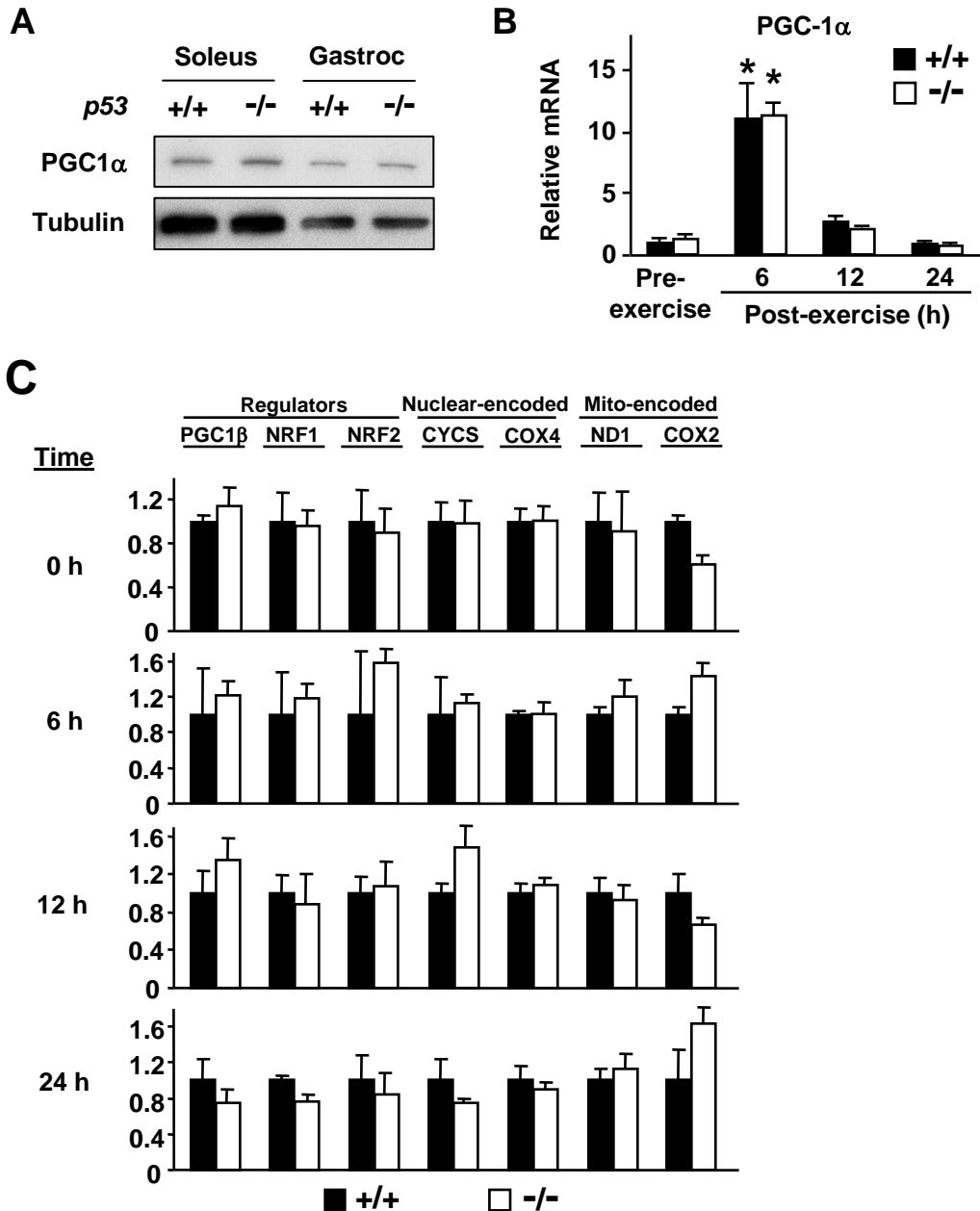
Online Figure III. Decreased mitochondrial density in *p53*^{-/-} mouse soleus muscle. A, Representative images of transmission electron micrographs of intermyofibrillar mitochondria in *p53*^{+/+} and *p53*^{-/-} mouse soleus muscles. Upper panel, 15000X; lower panel, 5000X. Scale bars, 1 μ m. B, Estimated relative volume density of mitochondria (%). **P < 0.01; n=3. Data shown as mean \pm SEM.

Online Figure IV



Online Figure IV. p53R2, SCO2, FDXR and TIGAR expression levels are unchanged by p53 genotype. A, SCO2 mRNA (left panel) and protein (right panel) expression levels in soleus of p53^{+/+} and p53^{-/-} mice. B, Relative p53R2 mRNA levels in soleus, heart and liver by RT-PCR. C, p53R2 protein expression in soleus, heart and liver tissues by western blotting. D, Relative FDXR (left panel) and TIGAR (right panel) mRNA levels. Tubulin levels are shown as protein loading control (A and C). p53^{+/+} (dark) and p53^{-/-} (light) mice; data shown as mean \pm SEM.

Online Figure V



Online Figure V. PGC-1 α , other mitochondrial biogenesis regulators and mitochondrial respiratory subunit gene expression are not significantly affected by *p53* genotype at baseline or after acute exercise. A, Basal PGC-1 α protein levels detected by western blotting in soleus and gastrocnemius (Gastroc) of *p53*^{+/+} and *p53*^{-/-} mice. The positive control mouse myoblast C2C12 cell protein lysate shows a strong band at 96 kDal as specified by the manufacturer. B, Time course of PGC-1 α mRNA expression in response to acute exercise in *p53*^{+/+} and *p53*^{-/-} soleus muscle. C, PGC-1 β , other biogenesis regulators, and representative nuclear and mitochondrial genome-encoded component mRNA levels are not significantly affected by *p53* genotype at baseline or after acute exercise. **P* < 0.05 versus *p53*^{+/+} pre-exercise; *n* = 3. *p53*^{+/+} (dark) and *p53*^{-/-} (light) mice; data shown as mean \pm SEM.